The Generalized Haldane (GH) model of genetic drift resolving the many paradoxes of molecular evolution

Yongsen Ruan[*,1], Xiaopei Wang[1], Mei Hou[1], Liying Huang[1], Wenjie Diao[1], Miles Tracy[1], Shuhua Xu[2], Zhongqi Liufu[1], Haijun Wen[*,1] and Chung-I Wu[*,1]

Affiliations

[1]State Key Laboratory of Biocontrol, Innovation Center for Evolutionary Synthetic Biology, School of Life Sciences, Sun Yat-sen University, Guangzhou 510275, China.

[2]Center for Evolutionary Biology, School of Life Sciences, Fudan University, Shanghai 200438, China.

*Corresponding authors: ruanys3@mail.sysu.edu.cn, wenhj5@mail.sysu.edu.cn, ciwu@uchicago.edu.

Abstract

Genetic drift, the random changes in frequencies of neutral variants, is the fundamental force of molecular evolution. However, the standard Wright-Fisher (WF) model of random sampling in population of size N only partially defines genetic drift with $1/N$ or $1/N_e$ (N_e being a function of varying N's). In parallel, JBS Haldane (1927) proposed the branching process for genetic drift, whereby each gene copy is transmitted to K descendants with the mean and variance of $E(K)$ and $V(K)$. Whereas N is externally imposed on the standard and modified WF models, the Haldane model can be generalized (hence, the GH model) for regulating N's internally as a function of $E(K)$. The determination of N, as well as the broader definition of genetic drift based on $V(K)$, enables the GH model to account for many paradoxes of molecular evolution. They include: i) Genetic drift may often become stronger as N becomes larger; ii) The two sexes experience drift differently; iii) Genetic drift operates on advantageous mutations is independent of N; iv) Irresolution and paradoxes emerge in multi-copy gene systems (viruses, mitochondria, etc.) whereby genetic drift happens within and between individuals. We show how a GH model can resolve these paradoxes that elude the WF models. By integrating their results, GH models may supplant the WF models of genetic drift for the ever more complex biological systems.

Introduction

Genetic drift is defined as the random changes in frequency of genetic variants (Crow and Kimura 1970; Hartl and Clark 1997; Lynch, et al. 2016). Much, or even most, of DNA sequence evolution is governed by the random drift of neutral mutations. Nevertheless, even non-neutral variants are subjected to genetic drift as advantageous mutations often have a small probability of being fixed. If the strength of genetic drift is under-estimated, random changes that are missed in the analysis would result in the over-estimation of other evolutionary forces of greater

biological interest, including selection, mutation, migration, meiotic drive and so on. In particular, the conclusion of pervasive selection at the molecular level has been suspected to be due to the failure to fully account for genetic drift (Crow and Kimura 1970; Fu 1997; Li 1997; Charlesworth 2009; Lynch, et al. 2016; Chen, Yang, et al. 2022).

Hagedoorn and Hagedoorn (1921) may be the first to suggest that random forces (accidents, for example) could impact long-term evolution. In the same decade, models of genetic drift were developed along two lines. The one approach that became widely adopted is the Wright-Fisher (WF) model (Crow and Kimura 1970; Hartl and Clark 1997), formalized by Fisher (1930) and Wright (1931). They define genetic drift to be due to the random sampling of genes. Thus, in generation transition, the variance in the frequency of a variant allele, x, would be

$$V(x) = \frac{x(1-x)}{f(N)} = \frac{x(1-x)}{N_e} \quad (1)$$

where N is the population size. (Here, we present the haploid model while a factor of 2 should be added to the diploid models.) The WF model has been modified in many directions (Wright 1969; Gillespie 1975; Eldon and Wakeley 2006; Chen, et al. 2017; Sackman, et al. 2019) whereby the effective population size, N_e, is used to accommodate various deviations from the ideal WF population. We shall refer to the original and modified models in the plural as the WF models.

At about the same time, JBS Haldane introduced the branching process to model genetic drift (Haldane 1927; Haldane 1932). In the Haldane model, each gene copy is independently transmitted to K descendants with the mean and variance of $E(K)$ and $V(K)$. Again, we present the haploid model, noting some added complexities with diploidy.

A key difference between the two approaches is the determination of N. In the WF models, N (and hence N_e) is supplied to the model externally. In contrast, the branching process of the Haldane model generates N internally by formulating N of the next generation as $N' = N \times E(K)$. While Haldane's model (1927) resets N' to N, we will present a Generalized Haldane (GH) model whereby $E(K)$ is negatively correlated with N, as is often observed in actual populations (Smith and Slatkin 1973; Sibly and Hone 2002). The GH model thus tracks gene frequency changes as well as regulates N.

In the Haldane model, $E(K)$ would determine the trajectory of N changes and $V(K)$ would determine the strength of genetic drift. Obviously, there is no drift if $V(K) = 0$. To scale drift at the population level, the variance becomes $V(K)/N$ (Kimura and Crow (1963); Chen, et al. (2017); see Supplement). In short, $V(K)$ is the reproductive component of genetic drift while $1/N$ is the sampling component or the scaling factor.

In the WF models, genetic drift is governed by $1/N_e$. Comparing the two models, one would

obtain $N_e = N/V(K)$ as has been derived for the WF models (Kimura and Crow 1963; Cannings 1974; Sjodin, et al. 2005; Der, et al. 2011). However, the mathematical equivalence is biologically untenable. First, N is not a constant and has to be supplied externally to the WF models whereas N is internally generated in the GH model. Second, $V(K)$ as a free variable is biologically untenable in the standard WF model whereby K should follow the Poisson distribution with $V(K) = E(K)$. Kimura and Crow (1963) noted the problem and suggested a mechanism akin to the branching process. These difficulties, shared by other models with population sampling (Moran 2008), will be explored further in Discussion in relation to sex-dependence drift.

Because the WF models neither track N nor model $V(K)$ biologically, several paradoxes of genetic drift emerge (see the overview below). In this study, we present a Generalized Haldane (GH) model that can resolve these paradoxes. As the wealth of results obtained by the WF model are often close approximations for the GH model, the integration of these results should facilitate the accurate quantitation of genetic drift in the ever more complex biological systems in the genomic era.

Results

Overview of the paradoxes of genetic drift

Among the paradoxes, a most curious one is genetic drift in relation to changing population size. The WF model dictates stronger drift when N is smaller. However, when N is very small (say, $N = 10$ in a bacteria or yeast population) and increases to 20, 40, 80 and so on, there is in fact little drift in this exponential phase. Drift will intensify when N grows to near the carrying capacity. This trend is the exact opposite of the tenet of the WF model. The second paradox concerns the genetic drift of sex-linked genes in relation to sex-dependent breeding successes (Charlesworth and Charlesworth 2000; Bachtrog 2013; Cortez, et al. 2014; Wilson Sayres, et al. 2014; Makova, et al. 2024). A third paradox is about drift strength when selection is also at work. A new mutation with a selective advantage would always be fixed if there is no random drift. With drift, fixation is probabilistic, but the probability does not depend on N or N_e. This curious property echoes the view that N or N_e is a scaling factor of drift, which is determined mainly by $V(K)$ (see Results).

The power of the Haldane model in resolving these paradoxes is the focus of this study. Furthermore, the companion study (Wang et al. 2024) addresses a fourth paradox – the evolution of multi-copy gene systems, whereby evolution proceeds in two stages - between as well as within individuals. Multi-copy gene systems including viruses, mitochondria, transposons and ribosomal genes, are hence beyond the power of the WF models. Broadly speaking, even diploidy is also multi-copy systems (Silver 1985; Wu, et al. 1988; Wu, et al. 1989; Lindholm, et al. 2016; Courret, et al. 2019).

On the Haldane model of genetic drift

In the original Haldane model, genetic drift is defined by the branching process (see Eq. (4) of Chen, et al. (2017)). Let K be the number of progenies receiving the gene copy of interest from a parent; K would follow the same distribution for all neutral variants. In haploids, K is equivalent to the progeny number of each parent. In diploids, K is the transmission success of each gene copy, which is separately tracked. By the Taylor approximations of the ratio of two variables (Kendall, et al. 2006), we obtain the approximation as

$$V(x) \sim \frac{x(1-x)}{N} \frac{V(K)}{E^2(K)} \qquad (2)$$

where x is the variant frequency (see Supplementary Information). This is the same approximation, when $V(K)$ is not very large, as obtained by the WF model (Kimura and Crow 1964; see Chen et al. 2017 for details). For Eq. (2), we provide further extensive simulations on the accuracy in both the fixation probability and fixation time of neutral variants (see Supplementary Information). The equivalence makes a simple point that, between the WF and Haldane models, the results are often shared even though the models are biologically very different. (Similarly, the diffusion and coalescence theories are also distinct approaches to the same population genetic phenomena.)

In the Haldane model, there would be no genetic drift if $V(K) = 0$, regardless of the value of N. When $E(K) = 1$ and N stays constant, we obtain

$$N_e = \frac{NE^2(K)}{V(K)} = \frac{N}{V(K)} \qquad (3)$$

Eq. (2) and Eq. (3) have been obtained for the WF model (Kimura and Crow 1963; Crow and Denniston 1988; Chen, et al. 2017). However, to permit $V(K) \neq E(K)$, the WF model would have to be modified to resemble the Haldane model (Kimura and Crow 1963; Caballero 1994). The issue will be revisited in Discussion.

Table 1 here

In **Table 1**, the data of progeny number from the literature indeed show over-dispersion in all taxa surveyed, i.e., $V(K) > E(K)$. In fact, $V(K) > 10\ E(K)$ can often be found, e.g., the ratio of $V(K)/E(K)$ among males of the mandrill (*Mandrillus sphinx*), the great reed warbler (*Acrocephalus arundinaceus*), and the rhesus macaque (*Macaca mulatta*) at 19.5, 12.6 and 11.3, respectively (Hasselquist 1995; Setchell, et al. 2005; Dubuc, et al. 2014). We have also found that $V(K)$ may be far larger than $E(K)$ in other biological systems such as viruses (Ruan, Luo, et al. 2021; Ruan, Wen, et al. 2021; Hou, et al. 2023).

I. The first paradox – The paradox of changing *N*

1. Empirical demonstration and simulation

This "paradox of changing *N*" is that "genetic drift increases when *N* increases". **Fig. 1a** shows the results in a cell culture in the exponential growth phase where each cell doubles every 13 hours. Hence, $V(K) \sim 0$ with almost no drift when *N* is as small as < 50. Genetic drift is expected to increase as *N* approaches the carrying capacity. The paradox is exemplified through computer simulations in **Fig. 1b-c**. These panels show the drift pattern in the Haldane model and the WF model, respectively, when the populations are growing as the logistic growth model (see Methods). In the WF model, the drift is strong initially but weakened as *N* increases. The pattern is reversed in the Haldane model. The contrast between the two panels is the paradox.

Fig. 1 here

To verify the simulations of **Fig. 1b-c**, we study the growth of yeast populations under laboratory conditions where cells appear to increase following the logistic growth curve. As shown in **Fig. 1d**, the lower portion of the S-curve portrays the exponential growth in a low-density population, while the upper curve indicates a slowdown in growth near the population's carrying capacity. We directly recorded the individual output (*K*) of each yeast cell in the early (n = 25) and late (n = 65) stage of population growth under real-time high-content fluorescence imaging (Methods).

It's evident that $V(K)$ is decoupled from $E(K)$. In the early stage, $E(K)$ is 10.04 with $V(K)$ = 0.60 over five one-hour intervals. In the high-density phase, $E(K)$ decreases to 2.83 but $V(K)$ increases to 1.09 in four intervals (**Fig. 1e-f**). Most interestingly, during the late stage of population growth, $V(\Delta K)$ (adjusted to the four-hour time span for comparison; see Methods) indeed increases as *N* increases (**Supplementary Table 3**). At the last time point, the population is closest to the carrying capacity and $V(\Delta K)$ experiences a substantial leap from around 1.12 to 1.82. Overall, the variance in progeny number $V(K)$ in a high-density population is always greater that in a low-density population (**Fig. 1g**). Indeed, $V(K)$ may exhibit an increase with the increase in *N*, sometimes outpaces the latter.

Measurements of these two growth phases demonstrate the "paradox of changing *N*" by showing i) there is almost no drift when *N* is very small; ii) as *N* increases, $V(K)$, hence, genetic drift would also increase. Furthermore, $V(K)$ may increase sharply when *N* is close to the carrying capacity. This trend appears to echo the field observations by Coltman, et al. (1999) who show that $V(K)$ increases more than 5-fold when *N* increases only 2.5-fold in the United Kingdom (UK) population of Soay rams (*Ovis aries*).

2. The density-dependent Haldane (DDH) model – A first attempt at the Generalized Haldane model

To explain the paradox of changing *N*, the model has to be able to track and regulate *N*.

Ironically, although the branching process can track the changes, the process has been deemed unsuitable for population genetics. This is because $N_t = N_0\ E(K)$^t would drive N to approach either zero or infinity as t becomes very large. Indeed, Haldane's original model reset N' to N in each generation. Any generalized Haldane (GH) model must take advantage of this feature by regulating N via $E(K)$, as attempted in this section.

The "paradox of changing N" can be explained by $N_e = N/V(K)$ if the numerator and denominator move in the same direction. Most interestingly, $V(K)$ may increase more than N itself. This has been shown when $V(K)$ is close to zero while N is growing exponentially. In addition, when N is very near the carrying capacity, even a small increase in N would intensify the competition and inflate $V(K)$. This is shown in the yeast experiment of **Fig. 1d** and supported by Coltman, et al. (1999) field study of ram populations in UK. Thus, the relationship between N and $V(K)$ may realistically lead to this paradox.

We now extend the Haldane model by incorporating density-dependent regulation of N in order to define the conditions of this paradox. The model developed here is on an ecological, rather than an evolutionary time scale. The simplest model of N regulation is the logistic equation:

$$\frac{dN}{dt} = rN\frac{C_k - N}{C_k} \quad (4)$$

with C_k being the carrying capacity. In the ecological time scale, a changing N would mean that the population is departing from C_k or moving toward it (**Fig. 2a**). (As will be addressed in Discussion, changing N in the WF model is depicted in **Fig. 2b** whereby N is at C_k. C_k may evolve too, albeit much more slowly in an evolutionary time scale.) Here, we consider changes in N in the ecological time scale. Examples include the exponential growth when $N \ll C_k$, seasonal fluctuation in N (Frankham 1995; Charlesworth 2009) and competition modeled by the Lotka-Volterra equations (Bomze 1983).

Fig. 2 here

Details of the DDH model are given in the Supplementary Information. A synopsis is given here: We consider a non-overlapping haploid population with two neutral alleles. The population size at time t is N_t. We assume that expected growth rate $E(K)$ is greater than 1 when $N < C_k$ and less than 1 when $N > C_k$, as defined by Eq. (5) below:

$$E(K_t) = \frac{E(N_{t+1})}{N_t} = \frac{r+1}{1 + r\left(\frac{N_t}{C_k}\right)^z} \quad (5)$$

The slope of $E(K)$ vs. N (i.e., the sensitive of growth rate to changes in population size), as shown in **Fig 3a**, depends on z. To determine the variance $V(K)$, we assume that K follows the

negative binomial distribution whereby parents would suffer reproduction-arresting injury with a probability of p_t at each birthing (Supplementary Information). Accordingly, $V(K)$ can then be expressed as

$$\frac{V(K_t)}{E(K_t)} = \frac{1-p_t}{p_t} = a(N_t)^b \quad (6)$$

By Eq. (6), the ratio of $V(K)/E(K)$ could be constant, decrease or increase with the increase of population size. With $E(K)$ and $V(K)$ defined, we could obtain the effective population size by substituting Eq. (5) and Eq. (6) into Eq. (3).

$$N_e = \frac{N_t E^2(K_t)}{V(K_t)} = \frac{N_t(r+1)}{a(N_t)^b\left[1 + r\left(\frac{N_t}{C_k}\right)^z\right]} \quad (7)$$

Eq. (7) presents the relationship between effective population size (N_e) and the population size (N) as shown in **Fig. 3**. The density-dependent $E(K)$ could regulate N with different strength (**Fig. 3a**). The steeper the slope in **Fig. 3a**, the stronger the regulation.

Fig. 3 here

The main results of this study are depicted in **Fig. 3b**. First, with no or little regulation of N, N_e and N are strongly correlated. The green dashed lines portray the conventional view of decreasing drift with increasing N. Second, under a particular strength of N regulation, the red line shows no dependence of N_e on N, meaning that genetic drift is independent of N. Finally, as N becomes strongly regulated, N_e and N would be negatively correlated as the blue dashed line shows. This trend is the paradox of changing N.

In summary, genetic drift effect can indeed decrease, increase or stay nearly constant as the population size increases, depending on the strength of N regulation near C_k. We further note that the $V(K)/E(K)$ ratio of Eq. (7) can be independent (**Fig. 3c**), positively dependent (**Fig. 3d**), or negatively dependent (**Fig. 3e**) on N. Interestingly, the results of **Fig. 3b** are nearly identical when the $V(K)/E(K)$ ratio changes (**Supplementary Figs 1-3**). These results show that the strength of genetic drift depends on the ecology that governs $E(K)$, $V(K)$ and N.

The paradox of changing N may not be an exception but a common rule in natural populations. Note that the WF approximation yielding Eq. (2) assumes nearly constant N. The assumption would imply very strong N regulation near C_k, which is precisely the condition leading to the paradox of changing N (**Fig. 3**). Coltman et al. (1999)'s observations of the reproduction in rams is such a case.

II. The paradox of genetic drift in sex chromosomes

Since the relative numbers of Y, X and each autosome (A) in the human population are 1:3:4, the WF model would predict the genetic diversity (θ_Y, θ_X and θ_A, respectively) to be proportional to 1:3:4. In a survey of human and primate genetic diversity, q_Y is almost always less than expected as has been commonly reported (Hammer, et al. 2001; Wang, et al. 2014; Wilson Sayres, et al. 2014; Makova, et al. 2024). The low θ_Y value has been used to suggest that human Y chromosomes are under either positive or purifying selection (Wang, et al. 2014; Wilson Sayres, et al. 2014; Makova, et al. 2024). Similarly, the reduced diversity X-linked genes was interpreted as a signature of positive selection (Pan, Liu, et al. 2022).

As pointed out above, under-estimation of genetic drift is a major cause of over-estimation of selective strength. Our goal is hence to see if genetic drift of different strength between sexes can account for the observed genetic diversities. Details will be presented in Wang et al. (2024). Below is a synopsis.

Let V_m and V_f be the $V(K)$ for males and females respectively and $\alpha' = V_m/V_f$ is our focus. (We use α' for the male-to-female ratio in $V(K)$ since α is commonly used for the ratio of mutation rate (Miyata, et al. 1987; Makova and Li 2002).) The three ratios, θ_Y/θ_X (denoted as R_{YX}), θ_Y/θ_A (R_{YA}) and θ_X/θ_A (R_{XA}), could be expressed as the functions of α', which incorporate the relative mutation rates of autosomes, X and Y (Supplementary Information). These relative mutation rates can be obtained by interspecific comparisons as done by Makova and Li (2002).

We note that there are many measures for the within-species genetic diversity, $\theta = 4N_e\mu$. Under strict neutrality and demographic equilibrium, these measures should all converge. In the neutral equilibrium, the infinite site model dictates the frequency spectrum to be $\xi_i = \theta/i$, where ξ_i is the number of sites with the variant occurring i times in n samples. Since every frequency bin is a measure of θ, different measures put different weights on the i-th bin (Fay and Wu 2000; Fu 2022). While p, the mean pairwise differences between sequences, is most commonly used in the literature, we use several statistics to minimize the possible influences of selection and demography (Wang et al. 2024). In this synopsis, we used the Watterson estimator (Watterson 1975) as the measure for θ_Y, θ_X and θ_A by counting the number of segregating sites.

Using any of the three ratios (θ_Y/θ_X, θ_Y/θ_A and θ_X/θ_A), we can obtain α'; for example, $R_{YA} = \theta_Y/\theta_A$ and, hence,

$$R_{YA} = \frac{y}{4}\frac{1+\alpha'}{2\alpha'}$$

where y is the mutation rate of Y-linked sequences relative to autosomal sequences. With rearrangement,

$$\alpha' = \frac{y}{8R_{YA} - y} \qquad (8)$$

Similar formulae of α' can be obtained for R_{YX} and R_{XA} but the accuracy for estimating α' is highest by R_{YA} whereas R_{XA} is the least accurate for this purpose (Supplementary Information).

Table 2 here

Table 2 presents the α' estimates in chimpanzees and bonobos. This is part of a general survey in mammals with a strong emphasis on primates and humans (Wang et al. 2024). It is almost always true that $\alpha' > 5$ in primates. Sources of data used are also given in **Table 2**. As shown for chimpanzees, α' is often far larger than 5, above which the resolution is very low as can be seen in Eq. (8). Note that, when R_{YA} is under-estimated and approaching $y/8$, α' would increase rapidly when the denominator is close to 0. That is why α' often becomes infinity (**Supplementary Fig. 5**). The estimated α' (MSE) in **Table 2** alleviates the problem somewhat by using all three ratios to calculate the mean square error (MSE) (Supplementary Information).

Among primates surveyed, bonobo is the only exception with $\alpha' < 1$. While chimpanzees and bonobos are each's closest relatives, their sexual behaviors are very divergent (de Waal 1995; De Waal and Lanting 2023). With unusually strong matriarchs, bonobo society seems to stand out among primates in sexual dominance. The α' value is important in behavioral studies and, particularly, in primatology and hominoid research. If 0.1% of males sire 100 children and the rest have the same K distribution as females, V_m/V_f would be ~ 10. Such outlier contribution is the equivalent of super-spreaders in viral evolution which may easily be missed in field studies. In this brief exposition, we highlight again that $V(K)$ or, more specifically, V_m and V_f are key to genetic drift. The differences in drift strength among X, Y and autosomes constitut a serious (but not immediately recognizable) paradox for the WF model as will be addressed in Discussion.

III. The paradox of genetic drift under selection

Genetic drift operates on neutral as well as non-neutral mutations. Let us assume a new mutation, M, with a frequency of $1/N$ is fixed in the population with the probability of P_f. Fisher (1930) first suggested that the fixation probability of an advantageous mutation should increase in growing populations, while decrease in shrinking populations. If there is no genetic drift (i.e., infinite population size in WF model), a beneficial mutation will always be fixed and $P_f = 1$. In the WF model, it is well known that $P_f \sim 2s$ for a new advantageous mutation, with fitness gain of s, while population size is large (Haldane 1932; Kimura 1962). This seems paradoxical that the determinant of genetic drift, $1/N_e$, does not influence P_f (Otto and Whitlock 1997; Lanfear, et al. 2014).

Fig. 4 here

In the Method section, we show that P_f under the Haldane model is given by

$$P_f = \sum_{t=0}^{\infty} \left[1 - \left(u_M(t)\right)^{M_0}\right] \left[\left(u_W(t)\right)^{W_0} - \left(u_W(t-1)\right)^{W_0}\right] \quad (9)$$

where M_0 and W_0 are the initial number of mutant allele (M allele) and wildtype allele (W allele), with $N = M_0 + W_0$. We note that $u_M(t)$ and $u_W(t)$, respectively, are the extinction probabilities of M allele and W allele by generation t with the initial number of alleles of 1. While obtaining the direct analytical solution of Eq. (9) may not be feasible, we could obtain its numerical solution due to its convergence as t increases (see Methods). The accuracy of the numerical solution from Eq. (9) is confirmed through simulation (**Supplementary Fig. 4**). Moreover, with the aid of the WF model (see Supplementary Information), we could obtain the approximation of Eq. (9) as follows.

$$P_f = \frac{2s}{V(K)} \quad (10)$$

We verify Eq. (10) by both the numerical solution from Eq. (9) and simulations based on the branching process (**Supplementary Fig. 4**). The fixation probabilities obtained by numerical solution vs. those inferred from Eq. (10) are shown in **Fig. 4**. The salient feature is that the fixation probability of $2s$, as in the classical formula, would be a substantial over-estimate when $V(K)$ is larger than $E(K)$. Eq. (10) is sufficiently accurate as long as $N \geq 50$. When N is as small as 10, the theoretical result is biased. Indeed, at such a low N value, the population is prone to extinction. The DDH model presented above should rectify this deficiency.

The main message of Eq. (10) is that genetic drift under positive selection is influenced by s and $V(K)$ but not by N. This independence from N seems intuitively obvious: when an advantageous mutation increases to say, 100 copies in a population (depending mainly on s), its fixation would be almost certain, regardless of N. This may be a most direct argument against equating genetic drift with N, or N_e (which is supposed to be a function of N's).

Discussion

Genetic drift should broadly include all random forces affecting evolutionary trajectories. While the standard WF model has been extended in several directions (overlapping generations, multiple alleles, ploidy, family size etc.) as presented in Introduction, many of these forces are still excluded from the WF models, thus resulting in the many paradoxes addressed here. The DDH model, the first GH model, can effectively resolve these paradoxes. We note that the original Haldane model suppresses N fluctuation and is hence a special case of DDH with extremely strong N regulation near C_k.

We shall first clarify the first paradox, the "paradox of changing N's". We note that the DDH model is on an ecological time scale whereby a population is either approaching or departing the carrying capacity (**Fig. 2a**). However, in many studies, the population size changes in the evolutionary time scale (**Fig. 2b**). For example, by the PSMC model (Li and Durbin 2011), both the European and Chinese populations experience a severe bottleneck 10-60 kyr ago. Presumably, various environmental forces may have reduced C_k drastically. Averaged over the long-time span, N should be at or near C_k. It should also be mentioned that the DDH model is about neutral processes and hence distinct from the concept of "genetic draft" involving selection and hitchhiking (Gillespie 2000, 2001).

When N changes in the WF models, it is usually in the evolutionary time scale like the aforementioned PSMC model. Strictly speaking, the WF models assume $N \sim C_k$ and changing N means changing C_k. In contrast, in the ecological time scale, N is either approaching or departing C_k. Because the WF models do not generates N from within the model, they cannot possibly address the paradox of changing N's. Furthermore, the WF models face basic problems in ecology. While a field biologist needs to delineate a Mendelian population and determine its size, N or N_e, one cannot know what the actual population being studied is by the WF models. Is it the fly population in an orchard being sampled, in the geographical region, or in the entire species range? In short, the WF population does not correspond to any physical entity. The Haldane model is an individual-output model (Chen, et al. 2017) whereby the "population" is the collection of individuals that may not conform to the delineation of a WF population.

The second paradox of sex-dependent drift is that, in the standard WF model, K should follow a Poisson distribution with $V(K) = E(K)$. As $E(K)$ is the same between sexes but $V(K)$ is different (generally $V_m > V_f$), clearly $V(K) = E(K)$ would not be feasible. The solution is to define N_e's by N/V_m and N/V_f , respectively for males and females (Kimura and Crow 1963; Cannings 1974; Lynch, et al. 1995; Sjodin, et al. 2005; Der, et al. 2011). The solution is problematic both biologically and mathematically. Biologically, it is not clear what sort of sampling scheme could yield $V(K) \neq E(K)$, let alone two separate $V(K)$'s with one single $E(K)$. Mathematically, given separate K distributions for males and females, it is unlikely that $E(K)$ could be 1, hence, the population would either explode in size or decline to zero. Since the population size, supplied externally, to the model is often constant (or at least well constrained), the behaviors of the WF models would contradict the inputs. In short, N regulation has to be built into the genetic drift model as the GH model does to avoid this paradox.

The third paradox of genetic drift is manifested in the fixation probability of an advantageous mutation, $2s/V(K)$. As explained above, the fixation probability is determined by the probability of reaching a low threshold that is independent of N itself. Hence, the key parameter of drift in the WF model, N (or N_e), is missing. This paradox supports the assertion that genetic drift is fundamentally about $V(K)$ with N being a scaling factor.

The fourth paradox is about the multi-copy gene systems such as viruses and rRNA genes covered in the companion study (Wang, et al. 2024). These systems evolve both within and between hosts. Given the small number of virions transmitted between hosts, drift is strong in both stages as shown by the Haldane model (Ruan, Luo, et al. 2021; Ruan, Wen, et al. 2021; Hou, et al. 2023). Therefore, it does not seem possible to have a single effective population size in the WF models to account for the genetic drift in two stages. The inability to deal with multi-copy gene systems may explain the difficulties in accounting for the SARS-CoV-2 evolution (Deng, et al. 2022; Pan, Liu, et al. 2022; Ruan, et al. 2022; Hou, et al. 2023; Ruan, et al. 2023).

As the domain of evolutionary biology expands, many new systems do not fit into the WF models, resulting in the lack of a genetic drift component in their evolutionary trajectories. Multi-copy gene systems are obvious examples. Others include domestications of animals and plants that are processes of rapid evolution (Diamond 2002; Larson and Fuller 2014; Purugganan 2019; Chen, Yang, et al. 2022; Pan, Zhang, et al. 2022; Wang, et al. 2022). Due to the very large $V(K)$ in domestication, drift must have played a large role. Somatic cell evolution is another example with “undefinable” genetic drift (Wu, et al. 2016; Chen, et al. 2017; Chen, et al. 2019; Ruan, et al. 2020; Chen, Wu, et al. 2022). The Haldane model, as an "individual output" model, can handle these general cases of genetic drift in non-WF populations.

The Haldane model and the WF model are fundamentally different approaches to random forces of evolution. Compared with the WF models of genetic drift, the Haldane model is more intuitive in depicting actual populations. The DDH model is an example of the Generalized Haldane model that regulates N. We thus hope to see further developments of GH models that, by integrating the results of the WF models, will quantify genetic drift more generally across biological systems.

Methods

Cell culture and image analysis. NIH3T3 cells, a fibroblast cell line that was isolated from a mouse NIH/Swiss embryo, were stably transfected with the fluorescent, ubiquitination-based cell cycle indicator (Fucci) (Sakaue-Sawano, et al. 2008) plasmid using Lipofectamine 3000 Transfection Reagent (Invitrogen) following the manufacturer’s specified instructions. The Fucci-labeled cells exhibited distinct fluorescent signals indicative of G1, S, and G2/M phases, represented by red, yellow, and green, respectively. NIH3T3-Fucci cell was derived from single-cell colony and cultured in DMEM supplemented with 10% Calf Bovine Serum and penicillin/streptomycin. All cells were maintained at 37□ with 5% CO_2. Subsequently, the cells underwent extended time-lapse imaging using high-content fluorescence microscopy (PerkinElmer Operetta CLS) equipped with a 10x objective lens. Images were captured hourly over a 100-hour period, and the analysis was conducted using ImageJ (Fiji) (Schneider, et al. 2012) to count the number of cells (**Supplementary Table 1**).

Yeast strain construction. Strains were constructed on the genetic background of *Saccharomyces cerevisiae* strain BY4741. A GFP or BFP fluorescent protein expression cassette, under the control of the TDH3 promoter, was inserted into the pseudogene locus YLL017W. Transformations followed a published protocol (Gietz and Schiestl 2007). Transformants were plated on synthetic complete medium without uracil (SC-Ura), and from these, single colonies were selected. Confirmation of replacements was achieved through PCR, and cassette verification was performed using fluorescence microscopy. Subsequently, the constructed strains were cultivated non-selectively in YPD medium (1% Yeast extract, 2% Peptone, 2% D-glucose) at 30 □ on a rotary shaker.

Estimation of *V*(*K*) and *E*(*K*) in yeast cells. To discern division events, even under high concentration, we conducted co-cultures of the GFP-yeast and BFP-yeast at ratios of 1:1 and 1:25, with the initial cell concentration of 0.1% and 12.5%, respectively. Then the yeast cells were then continuously imaged under high-content fluorescence microscopy (PerkinElmer Operetta CLS) for 10 hours with 1-hour intervals to observe the individual offspring of GFP-yeast. Yeast cells with a distinct offspring number (*K*) within the initial 5 hours (with the high-density group limited to the first 4 hours) were documented (**Supplementary Table 2**). Subsequently, the mean and variance of *K* for each cell were calculated across various time intervals as follows.

According to the law of total variance,

$$V(I_t) = E[V(I_t|I_{t-1})] + V[E(I_t|I_{t-1})] = V_{t-1,t}E[I_{t-1}] + E^2{}_{t-1,t}V[I_{t-1}]$$

where I_t is the offspring number at time t for an initial single cell (i.e., the total number of progeny cells for a single cell after t hours), as documented in **Supplementary Table 2**. And $E_{t\text{-}1,\,t}$ represents the average of offspring number after single time interval (1 hour here) for each single cell from time t-1 to time t, while $V_{t\text{-}1,\,t}$ is the corresponding variance. Utilizing the documented total cell count at time t (denoted by N_t), we could calculate the average of offspring number for a single yeast cell in a specific time interval, e.g., $E_{t\text{-}1,\,t} = N_t / N_{t\text{-}1}$ and $E[I_{t\text{-}1}] = N_t / N_0$. With some rearrangement,

$$V_{t-1,t} = \frac{V(I_t) - E^2{}_{t-1,t}V[I_{t-1}]}{E[I_{t-1}]} = \frac{V(I_t) - (N_t/N_{t-1})^2 V[I_{t-1}]}{N_{t-1}/N_0}$$

Applying the aforementioned equations, we observed that both $V_{t\text{-}1,\,t}$ (i.e., $V(K)$ within a one-hour interval) and $V(I_t)$ (i.e., the $V(K)$ from 0 to time t) for yeast cells under high density (12.5%) are generally greater than the values under low density (**Supplementary Table 3**). This suggests that the variance of offspring number in high-density conditions could be larger than that in a low-density context. It's noteworthy that the estimated value of $V_{t\text{-}1,\,t}$ could be less than zero (**Supplementary Table 3**), implying a very small variance in the number of

offspring. Furthermore, the occurrence of negative values for $V_{t\text{-}1,\,t}$ is more frequent under low density than high density, indicating the higher variance of offspring number in high density as previously suggested.

To show the variance of offspring number overtime, we also calculated the change of offspring number within successive one-hour intervals, denoted as $V(I_t - I_{t\text{-}1})$. This value is intricately linked to the variance of offspring overtime. To facilitate the comparison with the total variance from 0h to 4h, we set $V(\Delta K) = 4V(I_t - I_{t\text{-}1})$ to account for the four-hour time span.

Simulation of genetic drift in the Haldane model and the Wright-Fisher (WF) model. In both models, interactions between individuals are implicitly included through the dependency of the average number of offspring on population size, as defined by Eq. (5). This dependency leads to the logistic population growth, reflecting the density-dependent interactions. The initial population size is set to 4, with initial gene frequency (i.e., the frequency of mutant allele) of 0.5. And the carrying capacity is established at 100, 000, with $r = 1$ and $z = 1$. In WF model, the population size at next generation is $N_{t+1} = N_t \times E(K_t)$. Note if the calculated value of N_{t+1} is not an integer, we round it to the nearest whole number. The number of mutant alleles follows a binomial distribution, allowing the simulation of gene frequency overtime in WF model. For Haldane model, the number of offspring number is assumed to follow a beta-binomial distribution. The mean of offspring number $E(K_t)$ is obtained from Eq. (5). The variance $V(K_t)$ is obtained from Eq. (6) with parameters $a = 1/300$ and $b = 1.2$. Given the mean and variance of the beta-binomial distribution, we simulated the number of mutant alleles and population size overtime and then traced the gene frequency overtime.

Fixation probability of a new mutation in Haldane model. Here we obtain the fixation probability of advantageous mutation in Haldane model governed by a branching process. The Haldane model considers a well-mixed population of N_t haploid parents with only two types of alleles (W for wildtype, M for mutant). There is no migration and new mutations in this model. Each individual is assumed to independently reproduce in discrete and non-overlapping generation, $t = 0, 1, 2, \ldots$. Thus, the number of offspring per allele (also an individual in this haploid population) at any generation is represented by a set of identically and individually distributed random variables. In particular, the numbers of offspring of M and W alleles (denoted as K_M and K_W respectively) can be represented by following distributions.

$$P(K_M = k) = i_k \text{ for } k = 0, 1, 2, \ldots$$
$$P(K_W = k) = j_k \text{ for } k = 0, 1, 2, \ldots$$

For a particular distribution, we can obtain the average number of offspring as follows.

$$E(K_M) = \sum_{k=0} k \times i_k$$

$$E(K_W) = \sum_{k=0} k \times j_k$$

With the selection coefficient of s (0 for neutral mutation, positive for advantageous mutation, and negative for deleterious mutation) of M allele, average offspring number of M allele and W allele will follow the relationship.

$$E(K_M) = E(K_W)(1 + s)$$

Now, the evolution of the number of M allele (denoted as M_t) and the number of W allele (denoted as W_t) as time process is a branching process.

To compare Haldane model with WF model (the offspring number follows Poisson distribution with variance and mean equal to 1), we will set $E(K_W) = 1$, $E(K_M) = 1 + s$. And then let the offspring number follows a more general and realistic distribution (including negative binomial distribution (negBin), beta-binomial distribution (betaBin)), which can let the ratio of variance to mean range from 1 to a large number. (For simplicity, we let $V(K_M)/E(K_M) = V(K_W)/E(K_W)$.) Based on the branching process, we obtained the fixation probability M alleles (see Supplementary Information for more details on the derivation).

$$P_f = \sum_{t=0}^{\infty} \left[1 - \left(u_M(t)\right)^{M_0}\right]\left[\left(u_W(t)\right)^{W_0} - \left(u_W(t-1)\right)^{W_0}\right]$$

where

$$u_M(t) = P(M_t = 0|M_0 = 1) = \sum_{k=0}^{\infty} P(M_t = 0|M_{t=1} = k) = \sum_{k=0}^{\infty} i_k (u_M(t-1))^k$$

$$u_W(t) = P(W_t = 0|W_0 = 1) = \sum_{k=0}^{\infty} P(W_t = 0|W_{t=1} = k) = \sum_{k=0}^{\infty} j_k (u_W(t-1))^k$$

Note $u_M(t = 1) = P(K_M = 0) = i_0$, $u_W(t = 1) = P(K_W = 0) = j_0$. And both $\{u_M(t), t = 0, 1, 2, \ldots\}$ and $\{u_W(t), t = 0, 1, 2, \ldots\}$ are a bounded monotonic sequence. Thus, although we cannot obtain the direct analytical solution for P_f, we could easily obtain their numerical solution by iteration to the case when both $u_M(t)$ and $u_W(t)$ converge.

Acknowledgements

We thank Weiwei Zhai, Xionglei He for helpful comments. The work was supported by the National Natural Science Foundation of China (32150006, 32200493, 32293193, 81972691), the National Key Research and Development Projects of the Ministry of Science and

Technology of China (2021YFC2301300, 2021YFC0863400).

Competing interest statement. Authors declare that they have no competing interests.

References

Bachtrog D. 2013. Y-chromosome evolution: emerging insights into processes of Y-chromosome degeneration. Nat. Rev. Genet. 14:113-124.

Bomze IM. 1983. Lotka-Volterra equation and replicator dynamics: A two-dimensional classification. Biol. Cybern. 48:201-211.

Caballero A. 1994. Developments in the prediction of effective population size. Heredity (Edinb) 73 (Pt 6):657-679.

Cannings C. 1974. The latent roots of certain Markov chains arising in genetics: A new approach, I. Haploid models. Advances in Applied Probability 6:260-290.

Charlesworth B. 2009. Fundamental concepts in genetics: effective population size and patterns of molecular evolution and variation. Nat. Rev. Genet. 10:195-205.

Charlesworth B, Charlesworth D. 2000. The degeneration of Y chromosomes. Philos Trans R Soc Lond B Biol Sci 355:1563-1572.

Chen B, Shi Z, Chen Q, Shen X, Shibata D, Wen H, Wu CI. 2019. Tumorigenesis as the Paradigm of Quasi-neutral Molecular Evolution. Mol. Biol. Evol. 36:1430-1441.

Chen B, Wu X, Ruan Y, Zhang Y, Cai Q, Zapata L, Wu CI, Lan P, Wen H. 2022. Very large hidden genetic diversity in one single tumor: evidence for tumors-in-tumor. Natl. Sci. Rev. 9:nwac250.

Chen Q, Yang H, Feng X, Chen Q, Shi S, Wu CI, He Z. 2022. Two decades of suspect evidence for adaptive molecular evolution-negative selection confounding positive-selection signals. Natl. Sci. Rev. 9:nwab217.

Chen Y, Tong D, Wu CI. 2017. A New Formulation of Random Genetic Drift and Its Application to the Evolution of Cell Populations. Mol. Biol. Evol. 34:2057-2064.

Coltman DW, Smith JA, Bancroft DR, Pilkington J, MacColl AD, Clutton-Brock TH, Pemberton JM. 1999. Density-dependent variation in lifetime breeding success and natural and sexual selection in Soay rams. Am. Nat. 154:730-746.

Cortez D, Marin R, Toledo-Flores D, Froidevaux L, Liechti A, Waters PD, Grutzner F, Kaessmann H. 2014. Origins and functional evolution of Y chromosomes across mammals. Nature 508:488-493.

Courret C, Chang CH, Wei KH, Montchamp-Moreau C, Larracuente AM. 2019. Meiotic drive mechanisms: lessons from Drosophila. Proc Biol Sci 286:20191430.

Crow JF, Denniston C. 1988. Inbreeding and Variance Effective Population Numbers. Evolution 42:482-495.

Crow JF, Kimura M. 1970. An Introduction to Population Genetics Theory. New York: Harper & Row.

de Waal FB. 1995. Bonobo sex and society. Sci. Am. 272:82-88.

De Waal FB, Lanting F. 2023. Bonobo: The forgotten ape: Univ of California Press.

Deng S, Xing K, He X. 2022. Mutation signatures inform the natural host of SARS-CoV-2. Natl. Sci. Rev. 9:nwab220.

Der R, Epstein CL, Plotkin JB. 2011. Generalized population models and the nature of genetic drift. Theor. Popul. Biol. 80:80-99.

Diamond J. 2002. Evolution, consequences and future of plant and animal domestication. Nature 418:700-707.

Dubuc C, Ruiz-Lambides A, Widdig A. 2014. Variance in male lifetime reproductive success and estimation of the degree of polygyny in a primate. Behav. Ecol. 25:878-889.

Eldon B, Wakeley J. 2006. Coalescent processes when the distribution of offspring number among individuals is highly skewed. Genetics 172:2621-2633.

Fay JC, Wu CI. 2000. Hitchhiking under positive Darwinian selection. Genetics 155:1405-1413.

Fisher RA. 1930. The genetical theory of natural selection. Oxford, England: Clarendon Press.

Frankham R. 1995. Effective population size/adult population size ratios in wildlife: a review. Genetics Research 66:95-107.

Fu YX. 1997. Statistical tests of neutrality of mutations against population growth, hitchhiking and background selection. Genetics 147:915-925.

Fu YX. 2022. Variances and covariances of linear summary statistics of segregating sites. Theor. Popul. Biol. 145:95-108.

Gietz RD, Schiestl RH. 2007. High-efficiency yeast transformation using the LiAc/SS carrier DNA/PEG method. Nat Protoc 2:31-34.

Gillespie JH. 2000. Genetic drift in an infinite population. The pseudohitchhiking model. Genetics 155:909-919.

Gillespie JH. 2001. Is the population size of a species relevant to its evolution? Evolution 55:2161-2169.

Gillespie JH. 1975. Natural selection for within-generation variance in offspring number II. Discrite haploid models. Genetics 81:403-413.

Hagedoorn AL, Hagedoorn AC. 1921. The relative value of the processes causing evolution. In. The Hague: M. Nijhoff The Hague.

Haldane JBS. 1932. The Causes of Evolution. London: Longmans, Green and Company.

Haldane JBS. 1927. A mathematical theory of natural and artificial selection, part V: selection and mutation: Cambridge University Press.

Hallast P, Maisano Delser P, Batini C, Zadik D, Rocchi M, Schempp W, Tyler-Smith C, Jobling MA. 2016. Great ape Y Chromosome and mitochondrial DNA phylogenies reflect subspecies structure and patterns of mating and dispersal. Genome Res. 26:427-439.

Hammer MF, Karafet TM, Redd AJ, Jarjanazi H, Santachiara-Benerecetti S, Soodyall H, Zegura SL. 2001. Hierarchical patterns of global human Y-chromosome diversity. Mol. Biol. Evol. 18:1189-1203.

Hartl DL, Clark AG. 1997. Principles of Population Genetics. Sunderland, Massachusetts: Sinauer Associates.

Hasselquist D. 1995. Demography and Lifetime Reproductive Success in the Polygynous Great Reed Warbler. Japanese Journal of Ornithology 44:181-194.

Herman DM, Colwell MA. 2015. Lifetime reproductive success of Snowy Plovers in coastal northern California. The Condor 117:473-481.
Hou M, Shi J, Gong Z, Wen H, Lan Y, Deng X, Fan Q, Li J, Jiang M, Tang X, et al. 2023. Intra-vs. Interhost Evolution of SARS-CoV-2 Driven by Uncorrelated Selection-The Evolution Thwarted. Mol. Biol. Evol. 40.
Kendall MG, Stuart A, Ord JK, Arnold SF. 2006. Kendall's advanced theory of statistics. London: Edward Arnold London.
Kimura M. 1962. On the probability of fixation of mutant genes in a population. Genetics 47:713-719.
Kimura M, Crow JF. 1963. The measurement of effective population number. Evolution:279-288.
Krüger O, Lindström J. 2001. Lifetime Reproductive Success in Common Buzzard, Buteo buteo: From Individual Variation to Population Demography. Oikos 93:260-273.
Kuester J, Paul A, Arnemann J. 1995. Age-related and individual differences of reproductive success in male and female barbary macaques (Macaca sylvanus). Primates 36:461-476.
Lanfear R, Kokko H, Eyre-Walker A. 2014. Population size and the rate of evolution. Trends Ecol. Evol. 29:33-41.
Larson G, Fuller DQ. 2014. The Evolution of Animal Domestication. Annual Review of Ecology, Evolution, and Systematics 45:115-136.
Li H, Durbin R. 2011. Inference of human population history from individual whole-genome sequences. Nature 475:493-496.
Li W-H. 1997. Molecular evolution. Sunderland: Sinauer Associates Incorporated.
Lindholm AK, Dyer KA, Firman RC, Fishman L, Forstmeier W, Holman L, Johannesson H, Knief U, Kokko H, Larracuente AM, et al. 2016. The Ecology and Evolutionary Dynamics of Meiotic Drive. Trends Ecol. Evol. 31:315-326.
Lynch M, Ackerman MS, Gout JF, Long H, Sung W, Thomas WK, Foster PL. 2016. Genetic drift, selection and the evolution of the mutation rate. Nat. Rev. Genet. 17:704-714.
Lynch M, Conery J, Burger R. 1995. Mutation Accumulation and the Extinction of Small Populations. The American Naturalist 146:489-518.
Makova KD, Li WH. 2002. Strong male-driven evolution of DNA sequences in humans and apes. Nature 416:624-626.
Makova KD, Pickett BD, Harris RS, Hartley GA, Cechova M, Pal K, Nurk S, Yoo D, Li Q, Hebbar P, et al. 2024. The complete sequence and comparative analysis of ape sex chromosomes. Nature 630:401-411.
Miyata T, Hayashida H, Kuma K, Mitsuyasu K, Yasunaga T. 1987. Male-driven molecular evolution: a model and nucleotide sequence analysis. Cold Spring Harb Symp Quant Biol 52:863-867.
Moran PAP. 2008. Random processes in genetics. Mathematical Proceedings of the Cambridge Philosophical Society 54:60-71.
Nam K, Munch K, Hobolth A, Dutheil JY, Veeramah KR, Woerner AE, Hammer MF, Great Ape Genome Diversity P, Mailund T, Schierup MH. 2015. Extreme selective sweeps independently targeted the X chromosomes of the great apes. Proc Natl Acad Sci U S A

112:6413-6418.
Oring LW, Colwell MA, Reed JM. 1991. Lifetime reproductive success in the spotted sandpiper (Actitis macularia) : sex differences and variance components. Behav. Ecol. Sociobiol. 28:425-432.
Otto SP, Whitlock MC. 1997. The probability of fixation in populations of changing size. Genetics 146:723-733.
Pan Y, Liu P, Wang F, Wu P, Cheng F, Jin X, Xu S. 2022. Lineage-specific positive selection on ACE2 contributes to the genetic susceptibility of COVID-19. Natl. Sci. Rev. 9:nwac118.
Pan Y, Zhang C, Lu Y, Ning Z, Lu D, Gao Y, Zhao X, Yang Y, Guan Y, Mamatyusupu D, et al. 2022. Genomic diversity and post-admixture adaptation in the Uyghurs. Natl. Sci. Rev. 9:nwab124.
Purugganan MD. 2019. Evolutionary Insights into the Nature of Plant Domestication. Curr. Biol. 29:R705-R714.
Ribble DO. 1992. Lifetime Reproductive Success and its Correlates in the Monogamous Rodent, Peromyscus californicus. The Journal of Animal Ecology 61:457-468.
Ruan Y, Luo Z, Tang X, Li G, Wen H, He X, Lu X, Lu J, Wu CI. 2021. On the founder effect in COVID-19 outbreaks: how many infected travelers may have started them all? Natl. Sci. Rev. 8:nwaa246.
Ruan Y, Wang H, Chen B, Wen H, Wu CI. 2020. Mutations Beget More Mutations-Rapid Evolution of Mutation Rate in Response to the Risk of Runaway Accumulation. Mol. Biol. Evol. 37:1007-1019.
Ruan Y, Wen H, He X, Wu CI. 2021. A theoretical exploration of the origin and early evolution of a pandemic. Sci Bull (Beijing) 66:1022-1029.
Ruan Y, Wen H, Hou M, He Z, Lu X, Xue Y, He X, Zhang YP, Wu CI. 2022. The twin-beginnings of COVID-19 in Asia and Europe-one prevails quickly. Natl. Sci. Rev. 9:nwab223.
Ruan Y, Wen H, Hou M, Zhai W, Xu S, Lu X. 2023. On the epicenter of COVID-19 and the origin of the pandemic strain. Natl. Sci. Rev. 10:nwac286.
Sackman AM, Harris RB, Jensen JD. 2019. Inferring Demography and Selection in Organisms Characterized by Skewed Offspring Distributions. Genetics 211:1019-1028.
Sakaue-Sawano A, Kurokawa H, Morimura T, Hanyu A, Hama H, Osawa H, Kashiwagi S, Fukami K, Miyata T, Miyoshi H, et al. 2008. Visualizing spatiotemporal dynamics of multicellular cell-cycle progression. Cell 132:487-498.
Schneider CA, Rasband WS, Eliceiri KW. 2012. NIH Image to ImageJ: 25 years of image analysis. Nat Methods 9:671-675.
Setchell JM, Charpentier M, Wickings EJ. 2005. Sexual selection and reproductive careers in mandrills (Mandrillus sphinx). Behav. Ecol. Sociobiol. 58:474-485.
Sibly RM, Hone J. 2002. Population growth rate and its determinants: an overview. Philos Trans R Soc Lond B Biol Sci 357:1153-1170.
Silver LM. 1985. Mouse t haplotypes. Annu. Rev. Genet. 19:179-208.
Sjodin P, Kaj I, Krone S, Lascoux M, Nordborg M. 2005. On the meaning and existence of an

effective population size. Genetics 169:1061-1070.
Smith JM, Slatkin M. 1973. The Stability of Predator□Prey Systems. Ecology 54:384-391.
Wang CC, Jin L, Li H. 2014. Natural selection on human Y chromosomes. J Genet Genomics 41:47-52.
Wang X, He Z, Guo Z, Yang M, Xu S, Chen Q, Shao S, Li S, Zhong C, Duke NC, et al. 2022. Extensive gene flow in secondary sympatry after allopatric speciation. Natl. Sci. Rev. 9:nwac280.
Wang X, Ruan Y, Zhang L, Chen X, Shi Z, Wang H, Chen B, Tracy M, Wen H, Wu C-I. 2024. The paradox of extremely fast evolution driven in multi-copy gene systems - A resolution. In: eLife Sciences Publications, Ltd.
Watterson GA. 1975. On the number of segregating sites in genetical models without recombination. Theor. Popul. Biol. 7:256-276.
Wilson Sayres MA, Lohmueller KE, Nielsen R. 2014. Natural selection reduced diversity on human y chromosomes. PLoS Genet. 10:e1004064.
Wright S. 1969. Evolution and the Genetics of Populations, Volume 2: Theory of gene frequencies: University of Chicago press.
Wright S. 1931. Evolution in Mendelian Populations. Genetics 16:97-159.
Wu CI, Lyttle TW, Wu ML, Lin GF. 1988. Association between a satellite DNA sequence and the Responder of Segregation Distorter in D. melanogaster. Cell 54:179-189.
Wu CI, True JR, Johnson N. 1989. Fitness reduction associated with the deletion of a satellite DNA array. Nature 341:248-251.
Wu CI, Wang HY, Ling S, Lu X. 2016. The Ecology and Evolution of Cancer: The Ultra-Microevolutionary Process. Annu. Rev. Genet. 50:347-369.
Wysocki D, Jankowiak Ł, Cholewa M, Zyskowski D, Griffin A. 2019. Natal conditions, lifespan and lifetime reproductive success of European blackbirds. Behav. Ecol. 30:1707-1714.

Figures and Tables

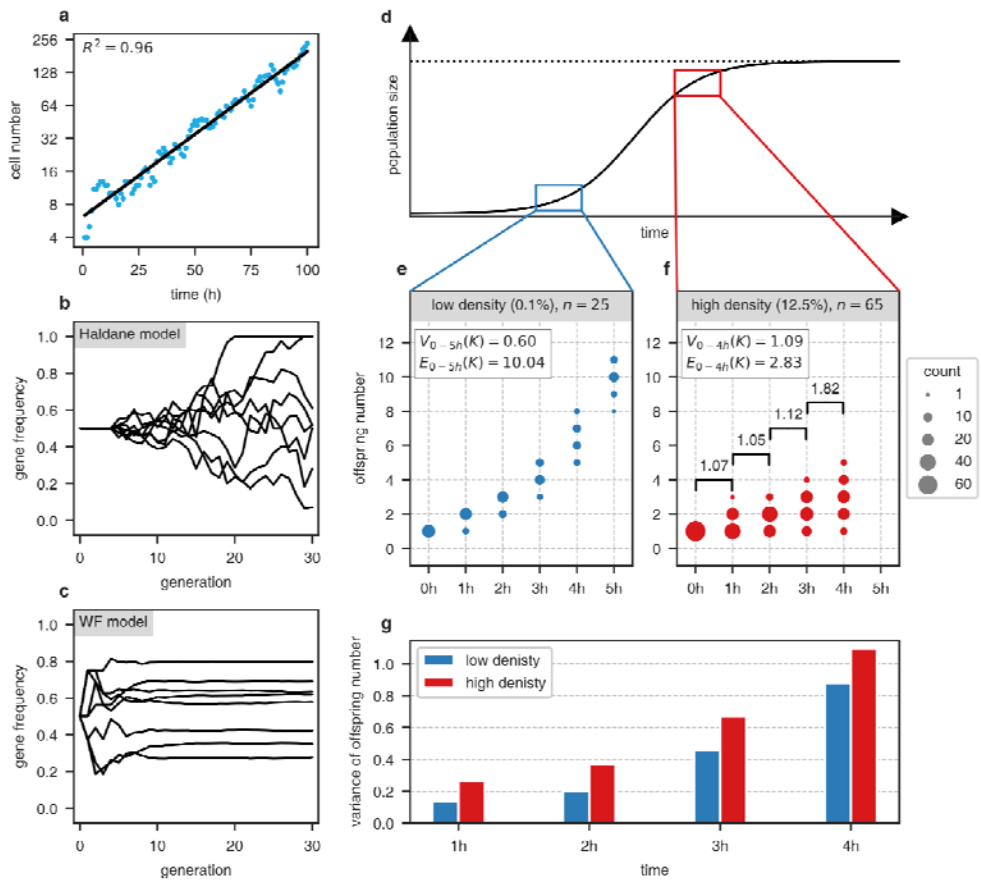

Fig. 1. The paradox of genetic drift when the population size (*N*) changes. (**a**) In the laboratory cell culture, nearly all cells proliferate when *N* is very small (interpreted in the next panel). (**b**) The simulation of Haldane model shows little genetic drift in the exponential phase. As in (a), drift may increase due to the heightened competition as the population grows. (**c**) Simulation by the WF model shows a pattern of drift opposite of the Haldane model. (**d**) The patterns of drift at the low and high *N* are analyzed in the framework of the logistic growth model. (**e-f**) Measurements of genetic drift in laboratory yeast populations at low and high density as defined in (d). The progeny number of each cell, *K*, is counted over 4 or 5 intervals as shown by the dots, the sizes of which reflect the cell number. $E(K)$ and $V(K)$ are presented as well. In panel (**f**), the change of offspring number overtime, denoted as $V(\Delta K)$, is shown above the braces. (**g**) The variance of offspring number $V(K)$ increases, observed in (e) and (f), as population size increases.

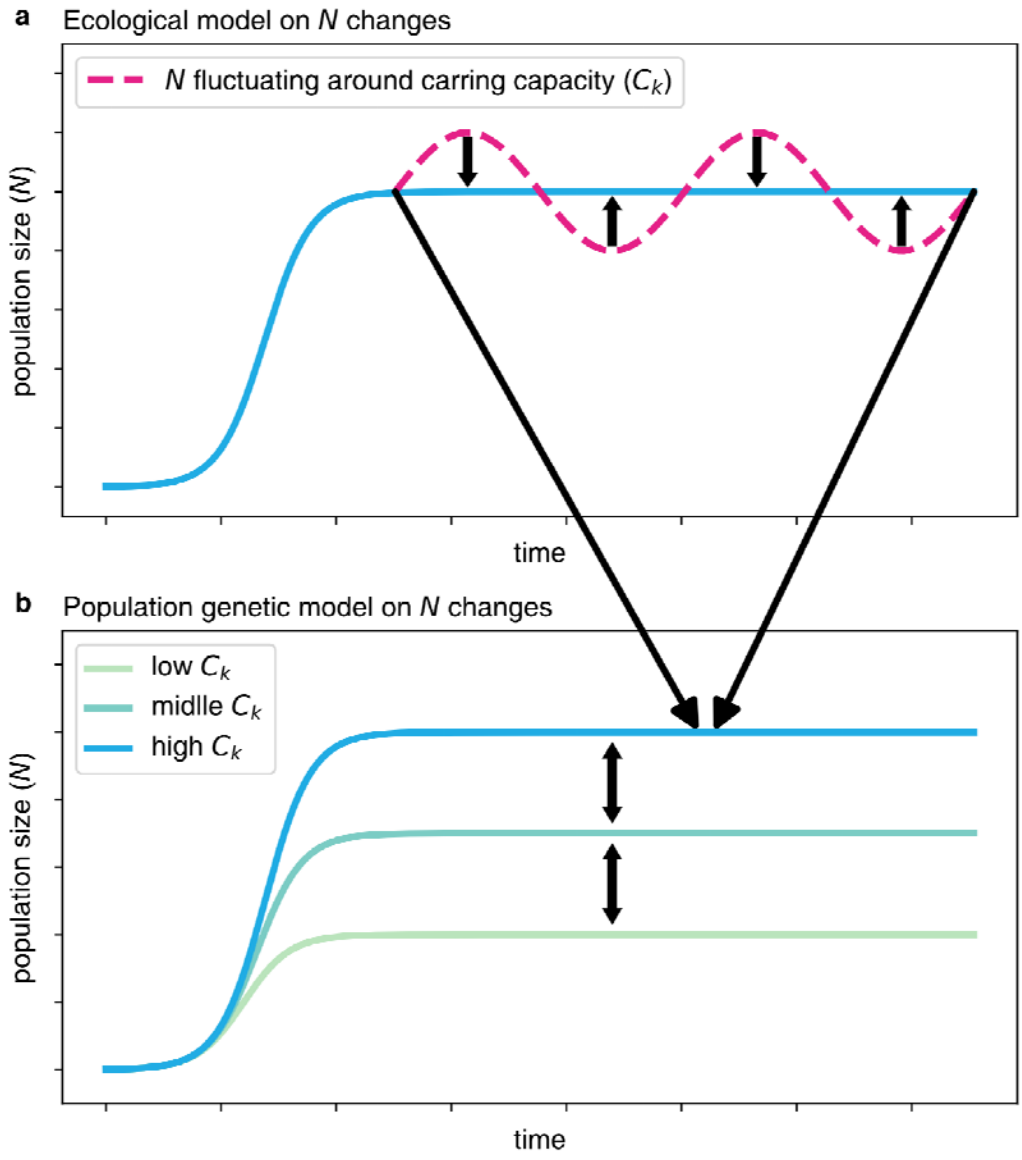

Fig. 2. The meaning of population size (*N*) changes in ecology vs. in population genetics. (**a**) In ecology, changing *N* would generally mean a population approaching or departing the carrying capacity. (**b**) In population genetics, a population of size *N* is assumed to be at the carrying capacity, C_k. Thus, changes in *N* would mean an evolving C_k, likely the consequence of environmental changes. The arrows indicate the disparity in time scale between the two scenarios.

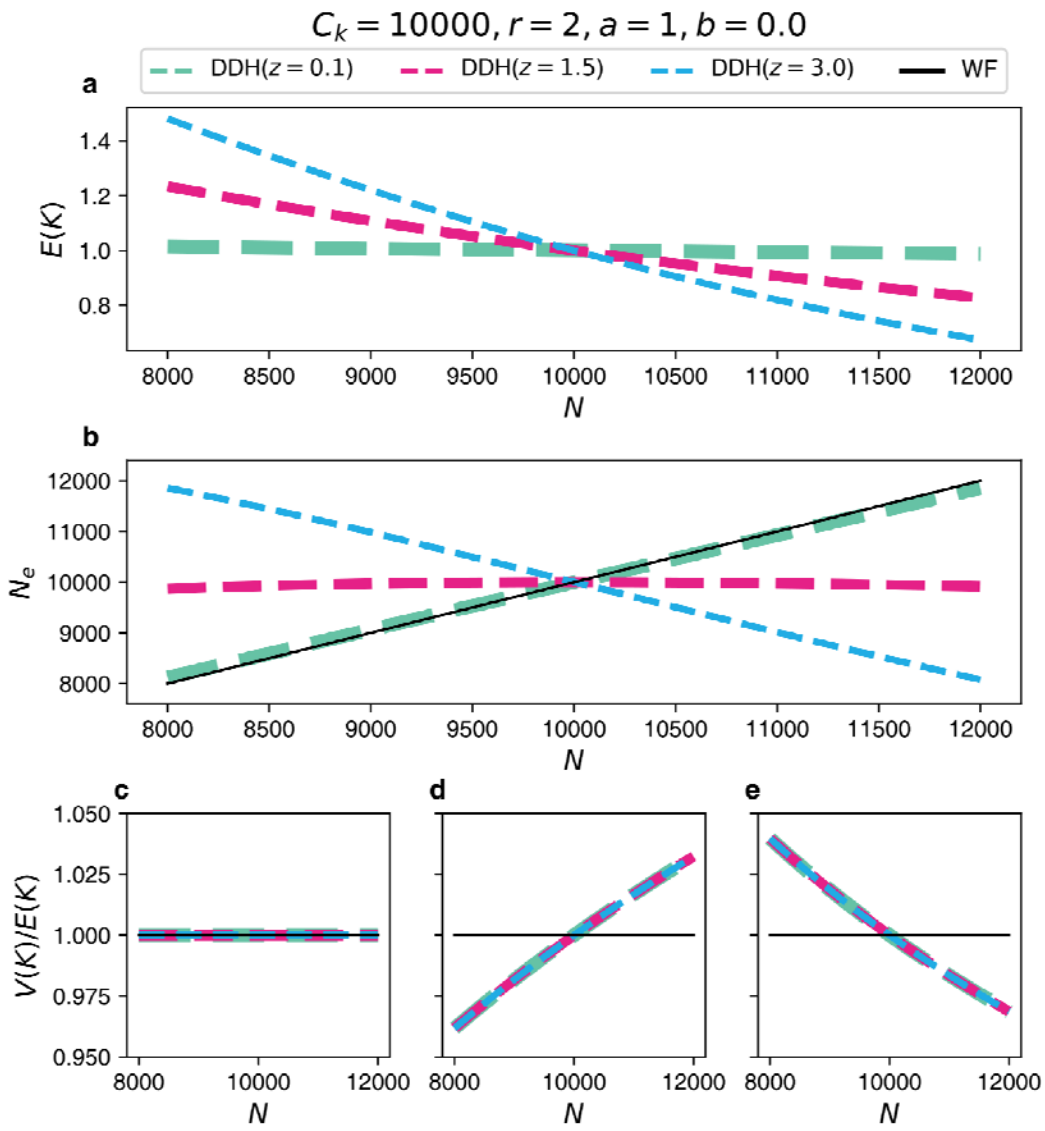

Fig. 3. Genetic drift as a function of population size in the DDH model. For all panels, the carrying capacity is C_k = 10,000 and the intrinsic growth rate is r = 2. (**a**) When N increases, $E(K)$ decreases as modeled in Eq. (5). The z value of Eq. (5) (0.1, 1.5 and 3) determines the strength of N regulation, indicated by the slope of $E(K)$ near C_k = 10,000. (**b**) Depending on the strength of N regulation near C_k, genetic drift can indeed decrease, increase or stay nearly constant as the population size increases. Thus, the conventional view of N_e being positively dependent on N is true only when the regulation of N is weak (the green line). At an intermediate strength (the red line), N_e is nearly independent of N. When the regulation becomes even stronger at z = 3, N_e becomes negatively dependent on N. (**c**-**e**) $V(K)/E(K)$ of Eq. (6)) is shown as a function of N. The results of panel (b) are based on a constant $V(K)/E(K)$ shown in panel (c). Interestingly, the results of panel (b) would not be perceptibly changed when $V(K)/E(K)$ varies, as shown in panel (d) and (e).

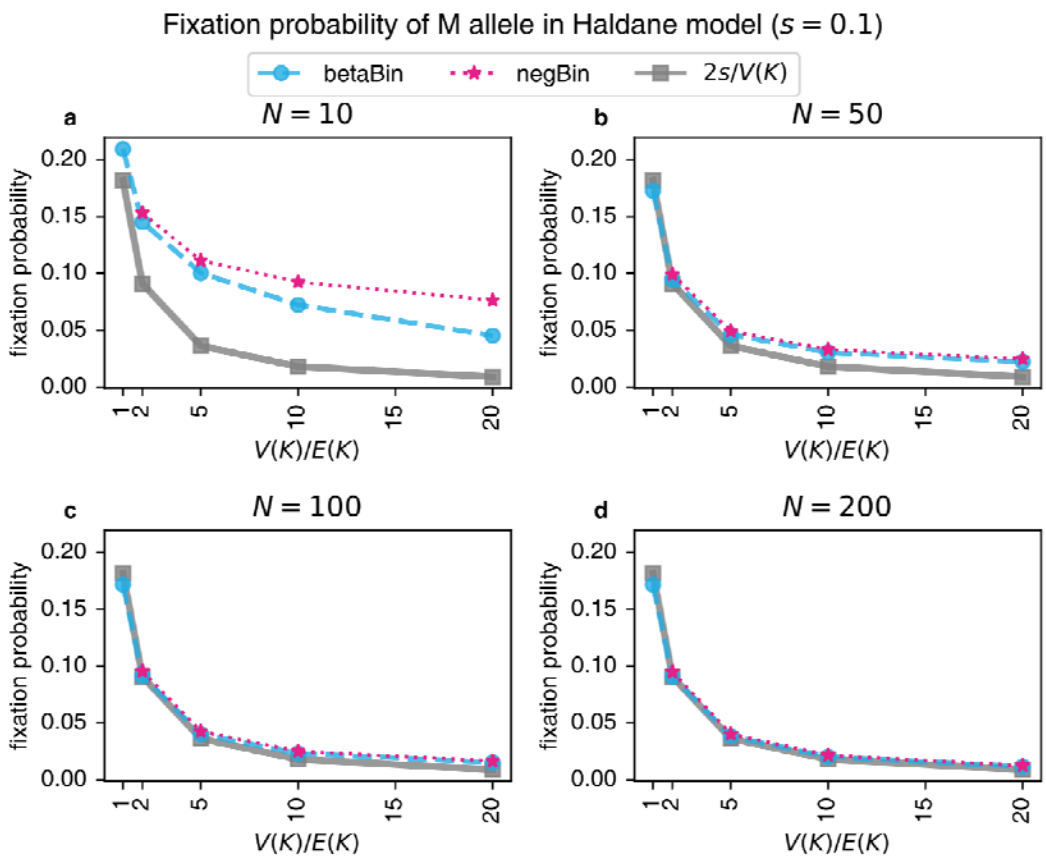

Fig. 4. Fixation probability of a new advantageous mutation in the Haldane model. The fixation probabilities of a new advantageous mutation with the selective advantage of $s = 0.1$ are calculated based on approximate solution from Eq. (9) (i.e., $2s/V(K)$) as well as numerical solution from Eq. (10). The numerical solution from Eq. (10) has been confirmed accurate by simulations (Supplementary Fig. 4). **(a-b)** When $N < 50$, the approximate fixation probability (the gray line) is lower than the simulated values (the color lines) due to population extinction. **(c-d)** By the Haldane model, the expected fixation probability of Eq. (9) is accurate when N reaches 100, as in most natural populations.

Table 1. Field record of $E(K)$ and $V(K)$ across diverse taxa.

Species	Type	Order	Gender	$E(K)$	$V(K)$	$V(K)/E(K)$	Sample Size	Literature
Macaca mulatta	Mammal	Primates	Female	7.7	15.4	2.0	132	Dubuc, et al. (2014)
			Male	8.7	98.7	11.3	86	
Mandrillus sphinx	Mammal	Primates	Female	4.7	19.8	4.2	51	Setchell, et al. (2005)
			Male	3.5	68.2	19.5	53	
Macaca sylvanus	Mammal	Primates	Female	1.2	2.9	2.4	98	Kuester, et al. (1995)
			Male	1.5	3.9	2.7	81	
Peromyscus californicus	Mammal	Rodentia	Female	4.7	7.7	1.6	16	Ribble (1992)
			Male	4.4	13.7	3.1	20	
Turdus merula	Bird	Passeriformes	Female	4.9	23.4	4.8	80	Wysocki, et al. (2019)
			Male	4.0	27.0	6.8	72	
Acrocephalus arundinaceus	Bird	Passeriformes	Female	7.7	53.3	6.9	82	Hasselquist (1995)
			Male	10.5	132.3	12.6	64	
Charadrius nivosus	Bird	Charadriiformes	Female	1.7	5.3	3.1	105	Herman and Colwell (2015)
			Male	2.2	9.0	4.1	90	
Actitis macularia	Bird	Charadriiformes	Female	5.2	26.9	5.1	66	Oring, et al. (1991)
			Male	3.3	17.2	5.2	103	
Buteo buteo	Bird	Accipitriformes	Female	3.5	13.8	4.0	106	Krüger and Lindström (2001)
			Male	2.7	9.3	3.4	132	

Table 2. Estimation of V_m/V_f in chimpanzee and bonobo.

	θ_Y ($\times 10^{-3}$)	θ_X ($\times 10^{-3}$)	θ_A ($\times 10^{-3}$)	α' (MSE)
Chimpanzee				
Western	0.034	0.533	1.623	4.98
Eastern	0.144	1.044	1.446	25.90
Nigeria-Cameroon	0.213	0.818	0.703	Inf [a]
Bonobo	0.492	0.446	0.867	0.57

Data for counting the segregating sites are from Hallast, et al. (2016) and Nam, et al. (2015).

θ_Y, θ_X, θ_A: genetic diversity for Y chromosome, X chromosome, and Autosomes (A), measured by Watterson estimator (Watterson 1975).

α' (MSE): optimal estimate for α' based on the minimum mean square error (MSE).

[a] Inf (infinity) designates cases when the estimated α' based on MSE is greater than 1000 (i.e., $V_m \gg V_f$).